Physics-Based Low-Frequency Noise Modelling in Small- and Large-Signal RF Device Operation

G. Conte, S. Donati Guerrieri, F. Bonani, G. Ghione

Politecnico di Torino, Dipartimento di Elettronica, Corso Duca degli Abruzzi 24,
10129 Torino, Italy, +390115644003, gabriele.conte@polito.it

Abstract— **The paper presents a generalized Green's function approach to the simulation of trap-assisted generation-recombination (GR) noise in RF devices. By exploiting a few noninteracting trap levels, the superposition of the corresponding (stationary) GR spectra is shown, in a simple yet significant case study, to reproduce a $1/f$ or $1/f$-like behaviour over a prescribed frequency range. The same trap distribution is also exploited for large-signal, cyclostationary noise simulations in forced periodic conditions. In this case, frequency conversion effects are present, and the low-frequency noise is shown to be upconverted from baseband to the other noise sidebands. The frequency conversion effects are also investigated in the case of a junction diode.**

I. Introduction

Trap assisted generation-recombination (GR) processes are known to play a significant role in the behaviour of advanced devices, both for MOSFETs where surface defects are responsible of degradation effects in the electron mobility, gate leakage etc., and in bipolars, where deep trap levels act as GR centers and are particularly important in the space-charge region. GR processes also give rise to noise due to charge fluctuations associated to carriers captured and emitted by the trap levels. Trap-assisted noise has been proposed as the underlying process giving rise to $1/f$ or $1/f$–like low frequency noise in some devices, such as the advanced MOS structures [1]. Since flicker noise can be modelled, on a certain frequency band, through a proper superposition of noninteracting GR spectra [2], a proper use of GR noise sources could also be a viable - though possibly empirical - substitute for a $1/f$ fundamental noise source, whose ultimate nature still appears to be elusive. Particular interest is related to the upconversion of low frequency GR noise to higher harmonics in large signal (LS) device operation. Such noise conversion mechanism is a well-known limiting factor in the RX-TX communication links. From the previous discussion, the importance of physics-based GR noise modelling not only in small-signal, but above all in large-signal conditions clearly emerges. While a full modelling approach to the nonlinear noise analysis for authonomous systems (oscillators, self-oscillating mixers) is still lacking [3], the nonlinear noise analysis in the non-authonomous case can be carried out by means of accurate physics-based simulations, thus leading to significant insight in the noise conversion mechanisms at the device level. In the present paper we present a comprehensive discussion on the physics-based simulation of GR noise originating from an arbitrary set trap-assisted processes within the framework of a drift-diffusion model. GR noise analysis is shown for two simple yet significant cases: a uniformly doped sample with nonlinear velocity-field relation (nonlinear semiconductor resistor) and a semiconductor pn junction.

The small-signal (stationary) and the large-signal (cyclostationary) cases are both discussed. For the uniformly doped sample the reconstruction of $1/f$ noise as a superposition of GR noise sources and their upconversion in the large-signal case are presented. For the diode case the upconversion of noise from the baseband to the upper sidebands demonstrates that the shape of the small signal spectrum is not simply upconverted in the large-signal case.

II. Noise modelling approach

The modelling of trap-assisted GR noise in semiconductor devices is based on the theory of population fluctuations described, e.g., in [4], [5]. We shall consider in this contribution the case of physics-based modelling carried out within the framework of the drift-diffusion transport model completed by a set of trap rate equations, expressing charge conservation, whose number corresponds to the total number of trap energy levels included in the simulation. Noise is modelled by adding to the conservation equations a stochastic forcing term, the *microscopic noise source*. The resulting model is:

$$\nabla^2\varphi = -\frac{q}{\epsilon}\left(p - n - \sum_{k=1}^{N} n_{\mathrm{t},k}\right) \tag{1a}$$

$$\frac{\partial n}{\partial t} = -\nabla\cdot\left(n\mu_n\nabla\varphi - D_n\nabla n\right) - U_n + \gamma_n \tag{1b}$$

$$\frac{\partial p}{\partial t} = \nabla\cdot\left(p\mu_p\nabla\varphi + D_p\nabla p\right) - U_p + \gamma_p \tag{1c}$$

$$\frac{\partial n_{\mathrm{t},k}}{\partial t} = -U_k + \gamma_k \qquad k = 1,\ldots,N \tag{1d}$$

where we have considered N trap levels ionized when filled by an electron. In the previous expressions φ is the electrostatic potential, n and p are the free carrier densities (electrons and holes, respectively), $n_{\mathrm{t},k}$ is the concentration of electrons filling trap-level k, q is the (positive) electron charge, ϵ is the material dielectric permittivity, μ is the carrier mobility and D the carrier diffusivity. $U = R-G$ is the net recombination rate of the energy level considered, R and G are the recombination and generation rates, respectively. Finally, γ are the stochastic forcing terms representing the microscopic noise sources.

Assuming non-interacting trap levels, the recombination and generation rates can be described according to the classical Shockley Read Hall model [6] originally derived for a single trap level. The free carrier GR rates are given by summation of the transition rates for the various traps:

$$R_n = \sum_{k=1}^{N} R_{n,k}; \quad G_n = \sum_{k=1}^{N} G_{n,k}$$
$$R_p = \sum_{k=1}^{N} R_{p,k}; \quad G_p = \sum_{k=1}^{N} G_{p,k}; \qquad (2)$$

where:

$$R_{n,k} = c_{n,k} n (N_{t,k} - n_{t,k}); \; G_{n,k} = c_{n,k} n_{1,k} n_{t,k}$$
$$R_{p,k} = c_{p,k} p n_{t,k}; \; G_{p,k} = c_{p,k} p_{1,k} (N_{t,k} - n_{t,k}) \qquad (3)$$

For the k-th trap level the GR rates are:

$$R_k = G_{n,k} + R_{p,k}; \quad G_k = R_{n,k} + G_{p,k} \qquad (4)$$

In (3) and (4), $N_{t,k}$ is the concentration of the k-th trap in the material, $c_{n,k}$ and $c_{p,k}$ are the capture coefficients, and the parameters $n_{1,k}, p_{1,k}$ are related to the trap energy level through the standard SRH formulation [6].

Physics-based noise analysis is carried out according to the well-known Green's function technique [5].

In the *stationary (small-signal) noise analysis*, the model equations are first solved in DC, without noise sources, to evaluate the noise-less steady-state. The microscopic noise sources are a small perturbation of the stationary steady state so that the model equations can be linearized around the DC working point. The microscopic fluctuations are then propagated to the device terminals by proper Green's functions, evaluated on the linearized model equations. Efficient numerical techniques, such as the generalized adjoint approach [5], can be exploited in order to reduce the computational burden of the Green's function evaluation. In the stationary case the *local noise source* corresponding to the correlation between the microscopic noise sources γ in (1) at the same spatial location is white, and given by[4], [5]:

$$\begin{aligned} K_{\gamma_n,\gamma_n} &= 2(R_{n0} + G_{n0}), \\ K_{\gamma_p,\gamma_p} &= 2(R_{p0} + G_{p0}), \\ K_{\gamma_k,\gamma_k} &= 2(R_{k0} + G_{k0}), \\ K_{\gamma_n,\gamma_k} &= -2(R_{n,k0} + G_{n,k0}), \\ K_{\gamma_p,\gamma_k} &= 2(R_{p,k0} + G_{p,k0}) \end{aligned} \qquad (5)$$

where index "0" means that all the transition rates are evaluated in the DC working point. The stationary short-circuit noise current generator correlation spectra are evaluated as a superposition integral of the local noise source and the propagation Green's functions [5]:

$$S_{\delta i_i,\delta i_j}(\omega) = \sum_{\alpha,\beta=n,p,k} \int_\Omega G_{i,\alpha}(\boldsymbol{r},\omega) K_{\gamma_\alpha,\gamma_\beta}(\boldsymbol{r}) G^*_{j,\beta}(\boldsymbol{r},\omega) \, \mathrm{d}\boldsymbol{r} \qquad (6)$$

where * denotes complex conjugate, while $G_{i,\alpha}(\boldsymbol{r},\omega)$ represents, at angular frequency ω, the Green's functions corresponding to injection in point $\boldsymbol{r}$ and equation α, and to observation on the short-circuit current at terminal i. Finally, Ω is the device volume.

Cyclostationary (large-signal) noise analysis is a generalization of the small-signal simulation technique. The main difference is due to the fact that the noiseless device working point is periodically time-varying, since it is determined by LS periodic or quasi-periodic generators. As a consequence, the stochastic processes describing fluctuations become cyclostationary, whose periodicity is the same as the LS working point [5], [7]. Cyclostationary processes exhibit correlation between those frequencies having the same distance from a frequency ω_k belonging to the LS periodic working point spectrum. This allows to partition the frequency axis into the *upper* ($\omega_k^+ = \omega_k + \omega$) and *lower sidebands* ($\omega_k^- = \omega_k - \omega$), where ω is the *sideband frequency* (limited to $\omega_0/2$ in the periodic case), while the statistical properties of the processes are described by a matrix, termed *sideband correlation matrix* (SCM), whose elements represent the correlation spectra between the various sidebands [5], [7].

In the cyclostationary case the microscopic noise sources are amplitude modulated by the device working point and converted into cyclostationary processes, whose SCM is:

$$(\mathbf{K}_{\gamma_n,\gamma_n})_{k,m} = 2(R_{n0,k-m} + G_{n0,k-m}), \qquad (7)$$

where $R_{n0,l}$ and $G_{n0,l}$ are the l-th harmonic components of the transition rates evaluated in the LS working point.

Furthermore, the propagation of the noise sources to the device terminals, as for the stationary case, is described by Green's functions defined on the model equations linearized around the working point. The linearized system is periodically time varying, so that propagation implies also frequency conversion effects. The SCM elements of the device terminal noise can be evaluated exploiting a generalization of (6):

$$\mathbf{S}_{\delta i_i,\delta i_j}(\omega) = \sum_{\alpha,\beta=n,p,k} \int_\Omega \mathbf{G}_{i,\alpha}(\boldsymbol{r};\omega) \cdot \mathbf{K}_{\gamma_\alpha,\gamma_\beta}(\boldsymbol{r};\omega) \cdot \mathbf{G}^\dagger_{j,\beta}(\boldsymbol{r};\omega)(\boldsymbol{r}) \, \mathrm{d}\boldsymbol{r}, \qquad (8)$$

where $\mathbf{G}_{i,\alpha}(\boldsymbol{r};\omega)$ is the conversion Green's function (CGF), which is now, for each injection point $\boldsymbol{r}$, a matrix expressing the possible conversion among sidebands, while $\dagger$ denotes hermitian conjugation. Numerical implementation of LS analysis is efficiently carried out in the frequency domain through the Harmonic Balance method [7]. Cyclostationary noise analysis is implemented according to the efficient CGFs evaluation technique described in [5], [7].

III. Case studies

In this contribution we investigate GR noise spectra in a two simple yet significant cases: a uniformly doped sample with nonlinear velocity-field relation (nonlinear semiconductor resistor) and a semiconductor pn junction.

First we consider a uniformly n doped Si sample, 2 μm long and with a cross section normalized to 1 cm^2, with doping level $N_D = 10^{16}$ cm^{-3}. The electron velocity field relation is described by the classical Caughey-Thomas model with low-field mobility $\mu_n = 1390$ cm^2 V^{-1} s^{-1} and saturation velocity 10^7 cm/s, while hole mobility is held constant to $\mu_p = 470$ cm^2 V^{-1} s^{-1}. The sample has been simulated by a 1D bipolar model properly extended to include the trap-level rate equations, implementing numerical noise analysis according to the model described in Sec. II.

$1/f$ noise spectrum has been shown to be obtained [2] over a finite frequency range from a superposition of noninteracting, single-level lorentzian GR noise spectra, where traps have the same energy levels while the capture coefficients must be chosen so as to yield timeconstants with a logarithmic distribution. This behaviour has been already verified by these

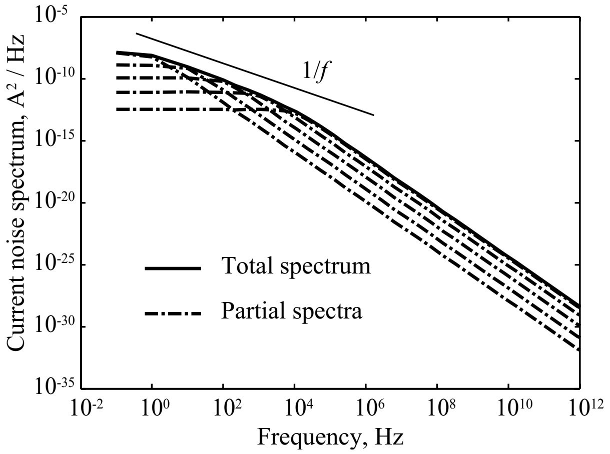

Fig. 1. Frequency dependence of the stationary GR current noise spectrum for 5 trap levels.

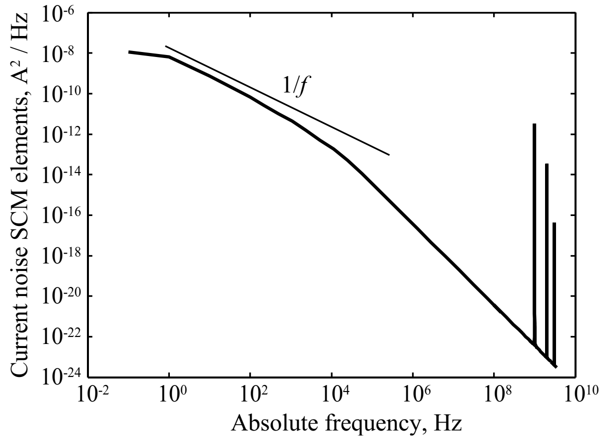

Fig. 2. Absolute frequency dependence of the diagonal elements for the GR current noise SCM for the sample with 5 trap levels.

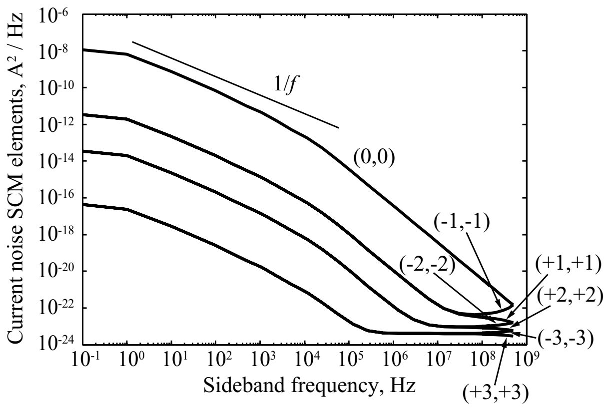

Fig. 3. Sideband frequency dependence of the diagonal elements for the GR current noise SCM for the sample with 5 trap levels.

authors in [8]. Since the presence of several trap levels with different timeconstants and the same energy level might be questionable in a real device, we have checked if it is possible to recover, at least approximately, $1/f$ noise behaviour in a prescribed frequency range by a superposition of trap noise spectra with different energy levels.

We have simulated the uniformely doped structure with 5 different trap energy levels with energies E_n =0.27, 0.24, 0.22, 0.21, 0.19 eV below the conduction band edge. In order to have partial GR noise spectra with corner frequencies logaritmically spaced in the 1 Hz and 10 kHz frequency range , the $c_n = c_p$ coefficients were chosen as: $c_n = 5.8 \times 10^{-12}, 5.1 \times 10^{-13}, 4.16 \times 10^{-14}, 3.6 \times 10^{-15}, 2.4 \times 10^{-16}$ cm^3/s. Fig. 1 presents the partial and total noise spectrum for this distribution of traps. In the required frequency range, the spectrum slope is slightly steeper than $1/f$, thus demonstrating that approximately $1/f$ spectrum can also be obtained within this modelling approach.

Concerning cyclostationary GR noise, we simulated the nonlinear resistor biased by a 2 V DC component plus a 0.2 V input tone at the frequency $f_0 = 1$ GHz. We included in the simulations 6 harmonics plus DC for the LS steady-state, thus allowing for the evaluation of the first 3 noise sidebands.

Frequency conversion of low-frequency noise is clearly observed in cyclostationary simulations, as shown in Fig. 2 and Fig. 3 where the diagonal elements of the short circuit current SCM are reported as a function of the absolute frequency and the sideband frequency, respectively. As expected in a resistor, stationary noise is upconverted with the same slope towards all the sidebands. This behaviour is in agreement with the results in [8] for a resistor with identical trap energy levels.

As a further example we shall consider a semiconductor pn junction. In this case the device is not uniform, so the single-trap small-signal noise spectrum is not a simple lorentzian any more; according to [6] the noise due to the presence of recombination centers in the space-charge region gives rise to a terminal spectrum made of two contributions: the first has a low-frequency behaviour and is found as the integral over the space charge region of local lorentizian spectra with corner frequency related to the SRH trap time costant; the second contribution is characterized by a costant behaviour at high frequency. Finally the two contributions are filtered by the RC filter composed of the diode junction capacitance and the parasitic resistance. The overall noise frequency behaviour is therefore much more complicated than the simple uniformly doped sample. Furthermore, the superposition of spectra from noninteracting traps may give rise to different frequency behaviour depending on the various physical parameters of the trap levels and the junction structure itself (doping, side lengths etc.). In this contribution we provide a preliminary analysis of noise in a test structure, in order to verify if the qualitative behaviour in [6] is confirmed and how the frequency dependency of the small-signal spectrum is converted to the harmonics in the LS case. The device we simulated is 10 μm long. The p and n sides are 5 μm long with costant doping $N_A = 10^{16}\,\mathrm{cm}^{-3}$ and $N_D = 10^{17}\,\mathrm{cm}^{-3}$. The electron and hole mobilities are field-independent: $\mu_n = 1390\,\mathrm{cm}^2/s$ and $\mu_p = 470\,\mathrm{cm}^2/s$. A single trap level is considered with $c_n = c_p = 5.7 \times 10^{-13}\mathrm{cm}^3/s$ and trap energy level at the middle of the energy gap. The device is forward biased with 0.5 V DC, in order to avoid high injection. Fig. 4 shows the small-signal short-circuit current noise spectrum. As predicted in [6] the frequency behaviour exhibits a quasi lorentzian spectrum and a costant plateaux at higher frequency, while at even higher frequencies a second cut is observed due to the filtering effect of the device itself. As expected, the device noise originates in the space-charge region, as shown in Fig. 5, where the integrand of the convolution integral (6) is plotted for two different frequencies. In the large signal case, with DC

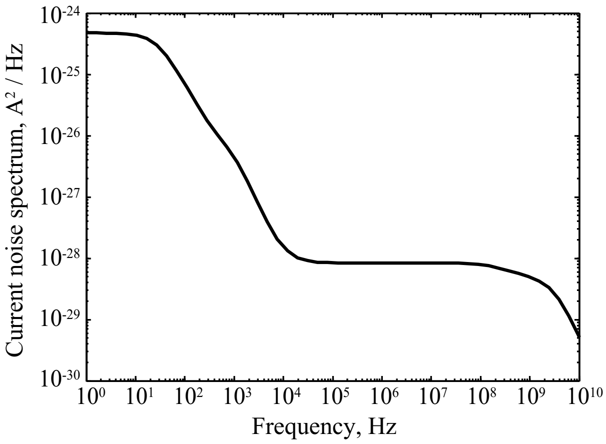

Fig. 4. Frequency dependence of the stationary GR current noise spectrum for the diode with a single trap energy level.

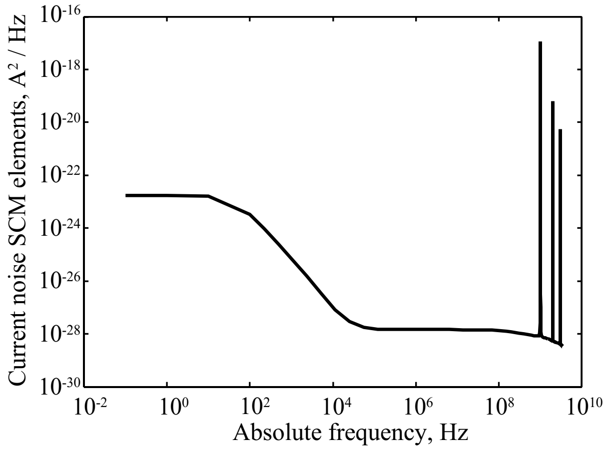

Fig. 6. Absolute frequency dependence of the diagonal elements for the GR current noise SCM for the juction diode.

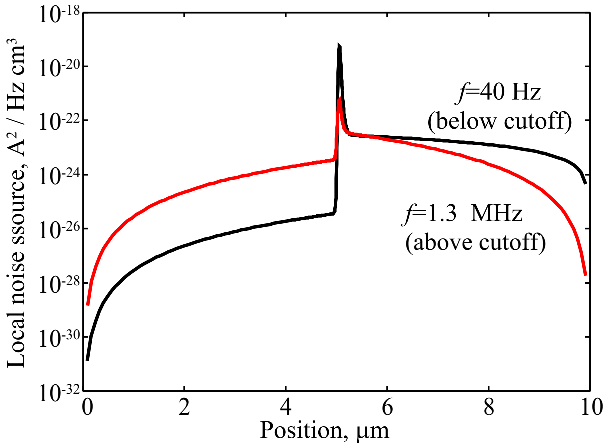

Fig. 5. Local noise contribution to diode short-circuit current noise spectrum at two different frequencies.

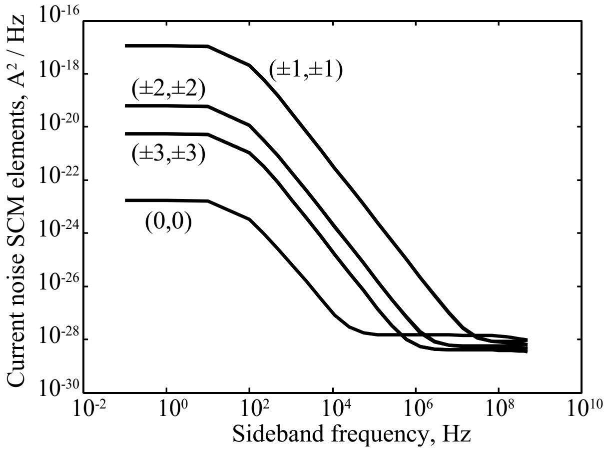

Fig. 7. Sideband frequency dependence of the diagonal elements for the GR current noise SCM for the juction diode.

plus a 0.05 V tone at 1 GHz, a strong conversion to higher frequency is observed, due to the diode nonlinearity in forward bias, as shown in Fig. 6. By inspecting the dependency of the diagonal elements of the SCM as a function of the sideband frequency, see Fig. 7, we observe that low-frequency noise is not simply upconverted with the same slope as the small-signal case: the frequency behaviour in the baseband differs from the small-signal one, showing that different frequency components are converted differently.

IV. Conclusion

A general approach to the trap assisted GR noise analysis both in the stationary and nonstationary case has been presented. Simulations have been carried out in two significant test cases: a nonlinear resistor with 5 noninteracting trap levels and a junction diode with a single trap level. In the first case the superposition of noise spectra is capable of providing a $1/f$ like frequency behaviour in the stationary case and, due to the uniform device structure, such noise is upconverted to the harmonics in the large-signal case with the same slope. In the diode case, noise originates in the space-charge region and yields a stationary noise which can exhibit lorentzian spectra, but these are not simply upconverted in the large signal case. This result poses limits in the possibilily of recovering exact $1/f$ noise upconversion in bipolar devices from the superposition of GR noise originated by deep trap levels.

Acknowledgement

This work was partially supported by the Italian Minister of University and Research through the PRIN 2003 project "Nonlinear noise models and design of low-phase noise oscillators for high performance communication systems".

References

[1] F. C. Hou, G. Bosman, M. E. Law, "Simulation of oxide trapping noise in submicron n-channel MOSFETs," *IEEE Trans. El. Dev.* **50,** No. 3, pp. 846–852, Mar. 2003.
[2] F. N. Hooge, "$1/f$ noise sources", *IEEE Trans. El. Dev.,* Vol. ED-41, No. 11, pp. 1926–1935, Nov. 1994.
[3] M. Odyniec, *RF and microwave oscillator design*, Artech House: Norwood, 2002.
[4] C. M. van Vliet, "Macroscopic and microscopic methods for noise in devices", *IEEE Trans. El. Dev.,* Vol. ED-41, pp. 1902–1915, Nov. 1994.
[5] F. Bonani, G. Ghione, *Noise in semiconductor devices: modelling and simulation*, Springer Verlag: Heidelberg, 2001.
[6] K. M. van Vliet, "Noise and Admittance of the Generation–Recombination Current involving SRH Centers in the Space–Charge Region of Semiconductor Devices", *IEEE Trans. El. Dev.,* Vol. ED-23, pp. 1236–1246, Nov. 1976.
[7] F. Bonani, S. Donati Guerrieri, G. Ghione, M. Pirola, "A TCAD approach to the physics-based modeling of frequency conversion and noise in semiconductor devices under large-signal forced operation", *IEEE Trans. El. Dev.*, Vol. ED-48, No. 5, p. 966, 2001.
[8] S. Donati Guerrieri, G. Conte, F. Bonani, G. Ghione, " Small and large signal trap-assisted GR noise modelling in semiconductor devices", *Proc. FaN 2004*, Vol. 5470, pp. 37–48, 2004.